S.T. Yau High School Science Award

Research Report

The Team

Name of team member: Jerry Fan
School: The Hotchkiss School
City, Country: Lakeville, CT, US

Name of supervising teacher: Yixiao Liu
Job Title: Ph.D. Student
School/Institution: Tsinghua University
City, Country: Beijing, China

Title of Research Report

Structural and Biochemical Characterization of an Adapter-Mediated Modular Ferritin Platform for EGFR-Targeted Glioblastoma Applications

Date

9/13/2026

Structural and Biochemical Characterization of an Adapter-Mediated Modular Ferritin Platform for EGFR-Targeted Glioblastoma Applications

Jerry Fan

Abstract

Glioblastoma multiforme (GBM) is an aggressive brain tumor marked by strong heterogeneity, frequent recurrence, and limited treatment efficacy, in part because the blood–brain barrier (BBB) restricts access of many therapeutics. Targeted therapy remains an attractive strategy, but it requires delivery systems that are both specific and experimentally tractable. Here we describe an adapter-mediated modular assembly strategy that enables post-assembly display of an EGFR minibinder on ferritin nanoparticles without redesigning the ferritin core itself. We first purified human ferritin heavy chain (FTH1) and confirmed that it self-assembles in solution. We then engineered a compact fusion adapter by linking the ferritin-binding region of NCOA4 to an EGFR minibinder through a flexible GS linker, and showed that the resulting bifunctional construct retains binding to both ferritin and EGFR. Finally, cryo-EM analysis of apo ferritin and the ferritin–fusion adapter complex provided structural support for efficient in vitro assembly. Taken together, these results define a biochemically and structurally validated ferritin platform for EGFR-directed applications relevant to GBM and support adapter-mediated assembly as a practical route for modular nanoparticle design.

Keywords: Glioblastoma multiforme (GBM), Ferritin nanoparticles, EGFR minibinder, Fusion adapter, Targeted drug delivery

Acknowledgement

This project was carried out by Jerry Fan under the academic guidance of Yixiao Liu. The research originated from Jerry's interest in protein engineering, nanobiotechnology, and targeted therapeutic strategies for glioblastoma. Through literature review and discussions with the instructor, the project focused on whether a receptor-targeting module could be introduced onto ferritin nanoparticles through an exchangeable adapter without directly redesigning the ferritin nanocage. Thanks Yixiao Liu for academic guidance and constructive discussions throughout the project. Thanks the laboratory safety personnel, facility staff, and technical personnel who provided laboratory access, safety supervision, and professional assistance with specialized instrumentation. Their support made the biochemical and structural characterization in this study possible.

Student Contribution

Jerry Fan was the principal student researcher and participated in the major stages of the research process. He conducted background research on glioblastoma, EGFR-targeted strategies, ferritin nanoparticles, NCOA4-mediated ferritin recognition, and computationally designed protein binders. With academic guidance, he participated in defining the research question and developing the strategy of linking an NCOA4-derived ferritin-binding region to an EGFR minibinder as a bifunctional adapter.

Jerry participated in planning and carrying out the experimental workflow, including recombinant protein preparation, purification and characterization, and interpretation of SDS–PAGE and negative-stain electron microscopy results. He also participated in the design and interpretation of surface plasmon resonance experiments evaluating the interactions of the fusion adapter with ferritin and EGFR. For cryo-electron microscopy, which requires specialized instrumentation and professional operation, qualified technical personnel provided instrument operation and/or data-acquisition support. Jerry's contribution focused on understanding the experimental design, comparing apo-ferritin and ferritin–adapter datasets, interpreting the reconstructed structures, and relating the structural observations to the biochemical results.

He also participated in structural prediction and model interpretation using computational tools, including AlphaFold3 and UCSF ChimeraX. He integrated the experimental results with relevant literature, organized the results and figures, developed the scientific interpretation of the project, and participated in preparing and revising the research report.

Instructor Contribution

Yixiao Liu served as the academic instructor for this project. He provided scientific and methodological guidance on the feasibility of the research question, experimental design, protein engineering strategy, laboratory procedures, interpretation of biochemical and structural results, and scientific presentation. He also discussed experimental difficulties and possible solutions with Jerry and provided feedback during revision of the research report. His role as the instructor was academic supervision and methodological guidance; the project report reflects Jerry's understanding of the research and his participation in the research process.

Commitments on Academic Honesty and Integrity

We hereby declare that we

1. are fully committed to the principle of honesty, integrity and fair play throughout the competition.
2. actually perform the research work ourselves and thus truly understand the content of the work.
3. observe the common standard of academic integrity adopted by most journals and degree theses.
4. have declared all the assistance and contribution we have received from any personnel, agency, institution, etc. for the research work.
5. undertake to avoid getting in touch with assessment panel members in a way that may lead to direct or indirect conflict of interest.
6. undertake to avoid any interaction with assessment panel members that would undermine the neutrality of the panel member and fairness of the assessment process.
7. observe the safety regulations of the laboratory(ies) where we conduct the experiment(s), if applicable.
8. observe all rules and regulations of the competition.
9. agree that the decision of YHSA is final in all matters related to the competition.

We understand and agree that failure to honour the above commitments may lead to disqualification from the competition and/or removal of reward, if applicable; that any unethical deeds, if found, will be disclosed to the school principal of team member(s) and relevant parties if deemed necessary; and that the decision of YHSA is final and no appeal will be accepted.

(Signatures of full team below)

X _____

Name of team member:

X _____

Name of supervising teacher:

Table of Contents

1. Introduction

2. Methods

2.1 DNA Construct

2.2 Protein Purification

2.3 Negative-Stain Electron Microscopy Sample Preparation and Data Collection

2.4 Surface Plasmon Resonance

2.5 Cryo-EM Sample Preparation and Data Collection

2.6 Cryo-EM Image Processing

2.7 Computational Structure Prediction and Model Docking

3. Results

3.1 Protein Purification and Validation of Nanocage Assembly

3.2 Binding Assays Support Bifunctional Target Engagement by The Fusion Adapter

3.3 Cryo-EM Confirms Assembly of the Ferrin-Adapter Complex

4. Conclusion

5. Discussion

1. Introduction

Glioblastoma (GBM) is the most common malignant brain tumor in adults and is characterized by rapid growth, extensive infiltration, and poor responsiveness to standard treatment [1,2]. Even with multimodal therapy, including surgery, radiotherapy, and chemotherapy, median survival is still less than 15 months [1,2]. Several features contribute to this poor outcome: marked intratumoral heterogeneity produces uneven treatment responses; invasive growth makes complete resection difficult; the blood–brain barrier (BBB) restricts delivery of systemically administered drugs; and GBM cells display multiple resistance mechanisms, including active efflux, efficient DNA damage repair, and tumor stem cell populations [1,2,3]. Together, these factors drive both recurrence and limited therapeutic benefit.

Targeted and immunotherapeutic approaches, including EGFR and VEGF inhibitors, CAR-T cells, and immune checkpoint blockade, have broadened the treatment landscape, but clinical benefit remains limited [2]. In practice, targeted agents often suffer from poor penetration, resistance caused by tumor heterogeneity, and off-target toxicity. Immunotherapies face additional barriers, such as the immunosuppressive brain microenvironment, limited T-cell infiltration, and tumor escape. For these reasons, there is still a strong need for delivery platforms that can be adapted for selective targeting in GBM.

EGFR is frequently amplified or mutated in GBM, and EGFRvIII is the best-known variant. This constitutively active form promotes proliferation, invasion, and therapy resistance. EGFR amplification and mutation are both closely associated with GBM malignancy and poor prognosis [4,5,6]. These features make EGFR an attractive target, although conventional monoclonal antibodies and small-molecule inhibitors have shown limited penetration and efficacy in the brain.

Ferritin is a highly conserved nanocage composed of 24 subunits and normally functions in iron storage and release. Its defined architecture, biocompatibility, and cargo-loading potential have made it an appealing scaffold for drug and gene delivery [7,8]. Ferritin can enter cells through receptor-

mediated endocytosis, and NCOA4 [9,10], a key regulator of ferritinophagy, binds ferritin and helps control intracellular iron handling. Most ferritin-targeting strategies decorate the particle surface directly, either by genetically fusing a targeting ligand to the ferritin subunit or by chemically modifying the assembled cage [11]. These approaches can work well, as illustrated by RGD-functionalized apoferritin for tumor targeting [12]. However, once the targeting module becomes larger or more complex, direct decoration can become difficult to optimize. Adjusting ligand copy number, spacing, or orientation often requires another round of construct redesign, while chemical coupling may introduce heterogeneity that complicates reproducibility and mechanistic interpretation [13]. A post-assembly strategy is therefore attractive, because it leaves ferritin self-assembly intact and allows the targeting component to be tuned separately through an exchangeable adapter.

Recent advances in de novo protein design have produced small, stable, high-affinity binders. Structure-guided and computational approaches can now generate EGFR binders that recognize tumor-associated receptors without relying on conventional antibodies or scFvs [14]. Deep-learning and diffusion-based methods have further accelerated this process [15]. These designed binders have already been incorporated into tumor-targeting systems such as CAR-T platforms, where they improve antigen recognition and cytotoxicity [16].

In this study, we asked whether GBM-relevant receptor targeting could be added to ferritin nanoparticles without repeatedly re-engineering the ferritin scaffold. To test this idea, we used human FTH1 as the nanocage and designed a separate NCOA4–EGFR minibinder fusion to serve as a bifunctional bridge. We then used SPR to examine whether this adapter retains binding to both ferritin and EGFR, and cryo-EM to assess whether the resulting assembly can be visualized structurally in vitro. The goal of this work is not to claim downstream delivery performance, but rather to establish an experimentally supported modular framework for EGFR-targeted ferritin display relevant to GBM.

2. Methods

2.1 DNA Construct

To construct FTH1, NCOA4, NCOA4-GSlinker-binder, the corresponding sequence was retrieved from the NCBI database or from prior study and cloned into the multiple cloning site of pGEX-6P-1 by homologous recombination. All constructs were verified by Sanger sequencing to confirm correct sequences.

2.2 Protein Purification

Recombinant fusion adapter, FTH1, and NCOA4(475–511) were expressed in E. coli BL21 (DE3). Protein expression was induced with isopropyl β-D-1-thiogalactopyranoside (IPTG) at a final concentration of 800 μM for 16 h. Cell lysates were first subjected to affinity purification using a GST–NTA column (GE Healthcare). The GST tag was subsequently removed by HRV3C protease prior to size-exclusion chromatography. The fusion adapter and NCOA4(475–511) were further purified using a Superdex 75 Increase 10/300 GL column (GE Healthcare), whereas FTH1 was purified using a Superose 6 Increase 10/300 GL column (GE Healthcare). All columns were equilibrated in buffer containing 50 mM Tris and 200 mM NaCl (pH 8.0). Protein purity was assessed by SDS–PAGE, and fractions corresponding to the major monodisperse peak were pooled, concentrated, and used for subsequent experiments. The protein was then concentrated to 2 mg/mL. Finally, all purified protein was flash-frozen in liquid nitrogen and stored at −80 °C.

2.3 Negative Stain EM Sample Preparation and Data Collection

For negative-stain electron microscopy, 5 μL of purified ferritin was applied to a freshly glow-discharged carbon-coated copper grid (300 mesh; Beijing Zhongjingkeyi Technology Co., Ltd.). After a 1 min incubation, excess sample was blotted away, and the grid was stained with 100 μL of 3% (w/v) uranyl acetate for 40 s. Excess staining solution was removed by aspiration, and the grids were air-dried at room temperature for 3 min prior to imaging. Micrographs were collected using the Tecnai Spirit T20 (Thermo Fisher Scientific, formerly FEI).

2.4 Surface Plasmon Resonance

Surface plasmon resonance (SPR) measurements were performed on a BIAcore 8K instrument (GE Healthcare, USA) at 25 °C using PBST buffer as the running buffer at a flow rate of 30 µL/min. Ferritin or EGFR proteins diluted in sodium acetate buffer (pH 4.0) were immobilized onto a CM5 sensor chip via standard amine-coupling chemistry. Serial concentrations of fusion adapter or NCOA4 proteins were injected over the immobilized surface to monitor binding responses. After each injection cycle, the sensor surface was regenerated using glycine–HCl solution (10 mM glycine, pH 1.5). Binding affinities were calculated, and sensorgrams were analyzed using BIAevaluation software (GE Healthcare, USA).

2.5 CryoEM Sample Preparation and Data Collection

For apo ferritin samples, 4 µL of purified ferritin was applied to a glow-discharged, carbon-coated copper grid (Cu 2/1 + 2 nm C, 300 mesh; Quantifoil) and incubated for 2 min. The grid was blotted for 6 s with a blot force of 0 under 100% relative humidity and plunge-frozen in liquid ethane using a Vitrobot Mark IV (FEI, USA).

For ferritin-adapter complex preparation, 5 µL of ferritin was first applied to an identically prepared grid and incubated for 2 min. Excess liquid was removed using filter paper, followed by addition of 3 µL of fusion adapter onto the same grid. The sample was incubated for an additional 3 min at 100% relative humidity before blotting for 4.5 s with a blot force of 0 and plunge-freezing in liquid ethane using a Vitrobot Mark IV (FEI, USA).

Cryo-EM data were collected on a 300 kV Titan Krios transmission electron microscope (FEI, USA) equipped with a K3 direct electron detector (FEI, USA). Automated data acquisition was performed using SerialEM. Movies were recorded at a calibrated magnification of 165,000×, corresponding to a pixel size of 0.68 Å per pixel, with a defocus range of −2.0 to −0.6 µm and a total electron dose of 50 $e^{-}/Å^{2}$.

2.6 CryoEM Data Processing

Movie frames were motion-corrected and dose-weighted using MotionCor2 [21]. Contrast transfer function (CTF) parameters were estimated with Patch CTF in cryoSPARC v4.4 [22]. A total of 257 micrographs for apo ferritin and 264 micrographs for the ferritin–adapter dataset were manually selected for further processing. All subsequent image analysis steps were carried out in cryoSPARC.

Templates for automated particle picking were generated from EMD-22657. In total, 83,626 particles were initially selected for apo ferritin and 67,889 for the ferritin–adapter dataset. Particles were extracted with a box size of 200 pixels (bin2). After multiple rounds of 2D classification, ab initio reconstruction, and heterogeneous refinement, 9,537 apo ferritin particles and 8,154 ferritin–adapter particles were retained for further analysis. These particles were then re-extracted with a box size of 400 pixels and subjected to non-uniform refinement with octahedral (O) symmetry, yielding final reconstructions at 3.33 Å and 3.55 Å for apo ferritin and the ferritin–adapter complex, respectively.

2.7 Structure Prediction and Docking

Structural prediction of the fusion adapter was performed using the AlphaFold3 [23] server. For model interpretation, the previously reported ferritin–NCOA4 complex structure [17] (PDB: 8QU9) together with the AlphaFold3-predicted EGFR minibinder model was docked into the cryo-EM density maps using UCSF ChimeraX. Model fitting was performed with the fit in map function, and density segmentation and visualization were carried out with the color zone tool in ChimeraX to assign individual structural components within the map.

3. Results

3.1 Protein Purification and Validation of Nanocage Assembly

To build a modular ferritin platform relevant to GBM, we first produced recombinant human ferritin heavy chain (FTH1) and asked whether it assembled correctly into nanocages in vitro. FTH1 was expressed in E. coli from a pGEX-6P-1 vector as an N-terminal GST fusion to improve solubility and enable affinity purification. After glutathione affinity chromatography and size-exclusion

chromatography (SEC), the GST tag was removed with HRV 3C protease and the sample was further polished by SEC. SDS–PAGE showed a major band at ~20 kDa, consistent with the expected size of FTH1. We then examined the purified protein by negative-stain electron microscopy. Micrographs collected on a 120 kV instrument showed mostly uniform spherical particles with an apparent diameter of ~11 nm and the expected hollow nanocage appearance, indicating that ferritin assembled properly and was suitable for subsequent engineering.

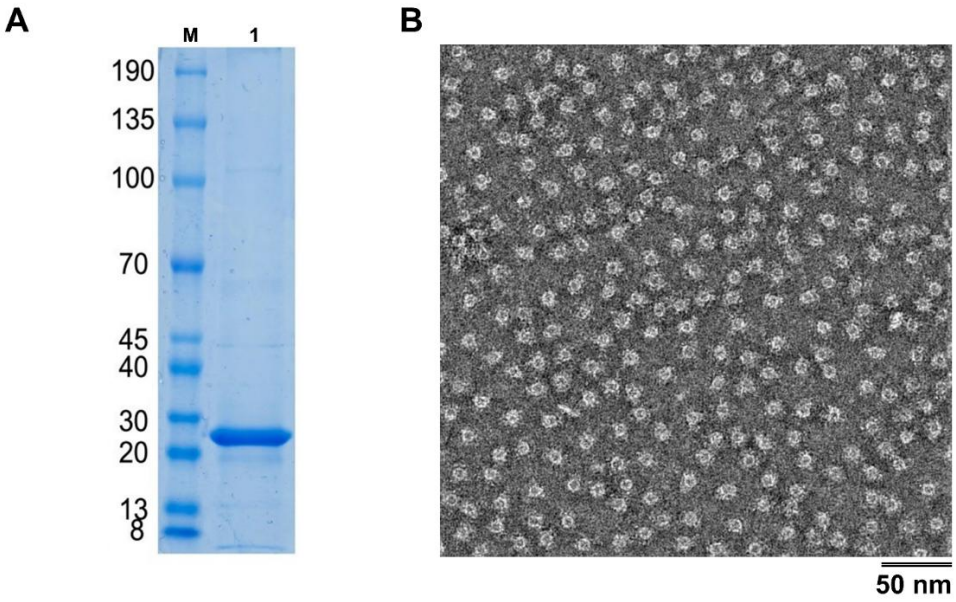


Figure 1. A) SDS-PAGE of Fth1. From left to right： marker, purified protein B) NS-staining EM verified the correct assembly of the ferritin nanoparticles

To introduce EGFR-directed targeting, we next designed a bifunctional adapter capable of bridging ferritin and receptor. The construct fused the native ferritin-binding region of NCOA4 to an EGFR minibinder [14] through a flexible GS linker so that the two binding functions could operate with minimal interference. To keep the adapter compact, NCOA4 was truncated to its minimal ferritin-binding segment (residues 475–511), which has previously been reported to be sufficient for ferritin recognition [17]. Because the final construct is small (103 amino acids), it was also expressed in E. coli as a GST fusion from pGEX-6P-1 and purified by affinity chromatography followed by SEC, with GST removed by HRV 3C protease. SDS–PAGE showed a prominent band at ~8 kDa and good purity,

indicating that the adapter can be produced cleanly for downstream assembly experiments. Structure prediction further suggested that the ferritin-binding motif and the EGFR-binding module adopt a separated arrangement, consistent with limited cross-talk between the two functions.

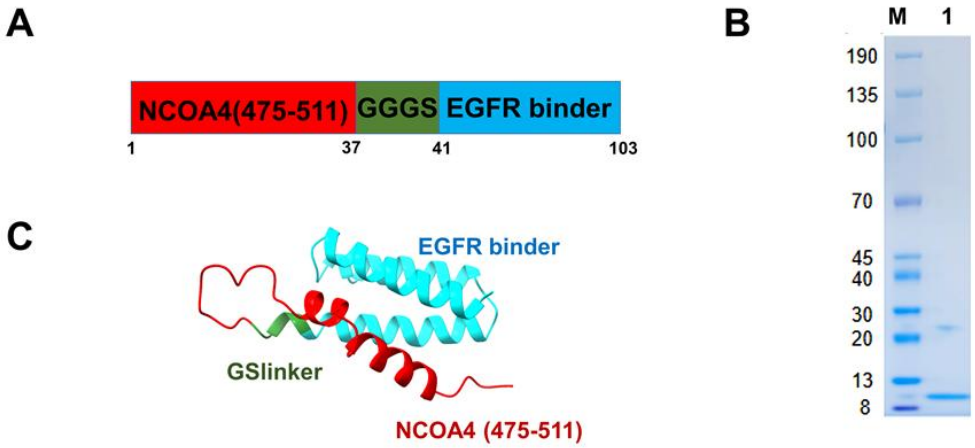


Figure 2. A) Sequence design for fusion adapter B) SDS-PAGE of NCOA4-GSlinker-binder From left to right： marker, purified protein C) Structure prediction for fusion adapter

3.2 Binding Assays Support Bifunctional Target Engagement by the Fusion Adapter

To quantify binding by the fusion adapter, we measured its affinity for ferritin and EGFR using surface plasmon resonance (SPR). As a control for ferritin binding, we also tested an NCOA4 fragment spanning residues 475–511. This NCOA4(471–511) construct was expressed and purified in the same way as the fusion adapter, and its purity was confirmed by SDS–PAGE. Because the affinity of the EGFR minibinder for EGFR has already been characterized in prior work, we did not repeat measurements for the standalone minibinder.

For the SPR experiments, ferritin and EGFR ectodomain (ECD) were immobilized on CM5 sensor chips, and increasing concentrations of either the fusion adapter or NCOA4(471–511) were injected to record binding responses. Sensorgrams were analyzed on a Biacore 8K with a 1:1 kinetic model to derive equilibrium dissociation constants (KD). The fusion adapter bound ferritin with a KD of 408 nM and bound EGFR ECD with a KD of 8 nM. By comparison, NCOA4(471–511) bound ferritin with a KD of 200 nM, whereas the reported affinity of the EGFR minibinder for EGFR is approximately 10 nM [14].

Fusion to the minibinder therefore caused only a modest reduction in ferritin binding, while preserving the same overall affinity range. Together, these data indicate that the GS-linked adapter retains binding to both ferritin and EGFR and can function as a bifunctional bridge for assembly of EGFR-targeted ferritin nanoparticles.

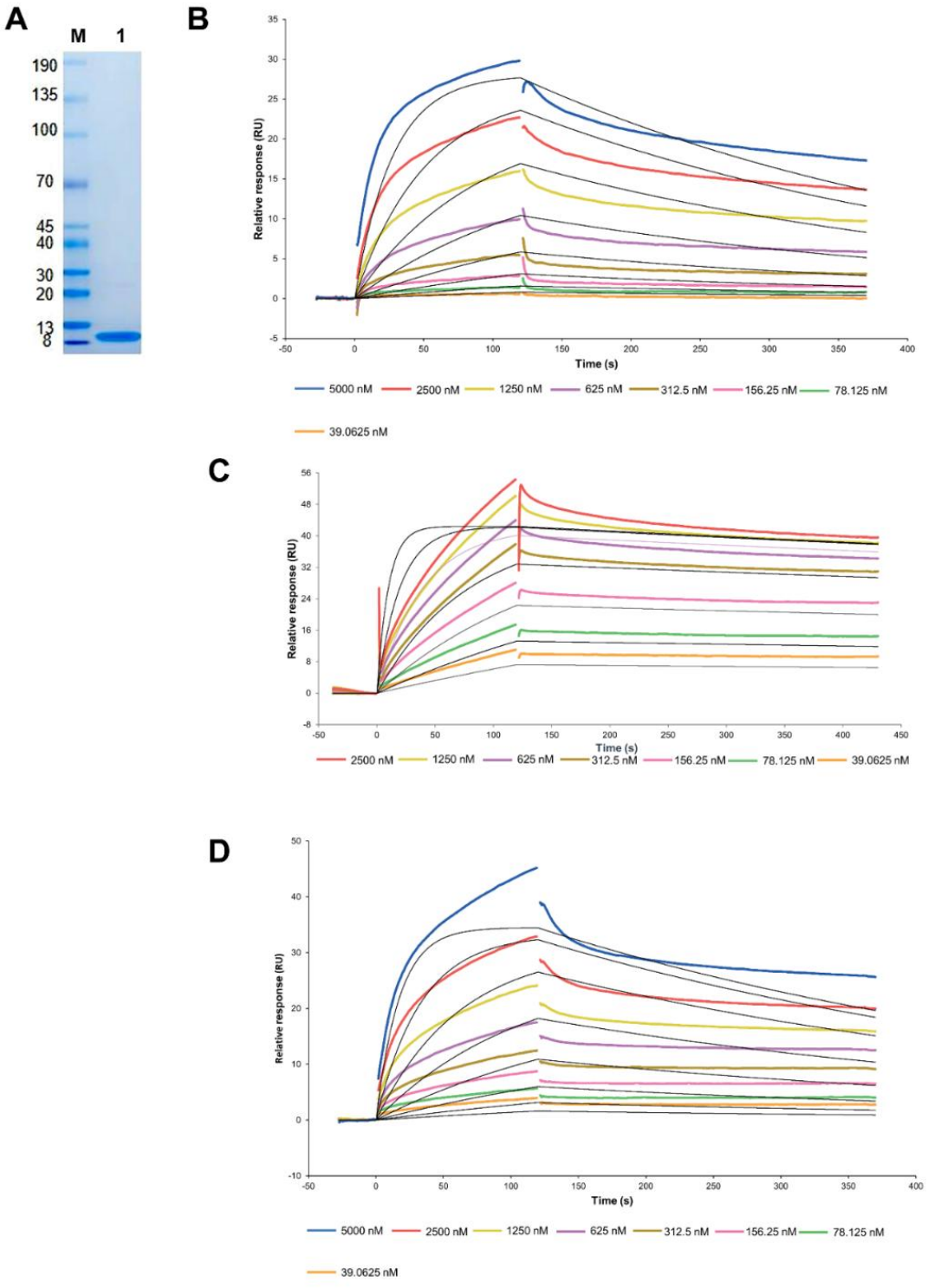


Figure 3. A) SDS-PAGE of NCOA4(475-511) From left to right：marker, purified protein B) Determination of the binding affinity between Ferritin and NCOA4-GSlinker-binder. Binding affinity was determined by BIAcore 8K sensorgrams. The concentrations of the analytes are indicated with different colors in each panel C) Determination of the binding affinity between EGFR and NCOA4-GSlinker-binder. Binding affinity was determined by BIAcore 8K sensorgrams. The concentrations of the analytes are indicated with different colors in each panel. D) Determination of the binding affinity between Ferritin and NCOA4(475-511) Binding affinity was determined by BIAcore 8K sensorgrams. The concentrations of the analytes are indicated with different colors in each panel. RU, resonance units.

3.3 Cryo-EM confirms assembly of the ferritin–adapter complex

Although the binding data showed that the fusion adapter engages ferritin with favorable affinity, we still needed to determine whether the two components form a stable complex in vitro, which is essential for a targeted ferritin platform. We therefore used cryo-electron microscopy (cryo-EM) to analyze apo ferritin and the ferritin–fusion adapter complex. Datasets were collected on an FEI Titan Krios G3, yielding 257 micrographs for apo ferritin and 264 micrographs for the ferritin–fusion adapter sample. Because the adapter is small, no clear difference was visible at the raw micrograph level. However, after particle picking and 2D classification, class averages from the ferritin–fusion adapter dataset showed weak diffuse density on the outer surface of ferritin that was absent from apo ferritin, consistent with bound adapter. We then curated particles in cryoSPARC and performed 3D reconstruction. Refinement with octahedral (O) symmetry produced maps at 3.33 Å for apo ferritin and 3.55 Å for the ferritin–fusion adapter complex.

Table 1 cryoEM data collection and processing

Data collection and processing	**Apo ferritin**	**Ferritin-adapter**
Magnification	165,000	165,000
Voltage (kV)	300	300
Electron exposure (e^{-}/Å^2)	50	50
Defocus range (μm)	-0.6 to -2.0	-0.6 to -2.0
Pixel size (Å)	0.68	0.68
Symmetry imposed	O	O
Initial particle images (no.)	83,626	67,889
Final particle images (no.)	9,537	8,154
FSC threshold	0.143	0.143
Resolution	3.33	3.55

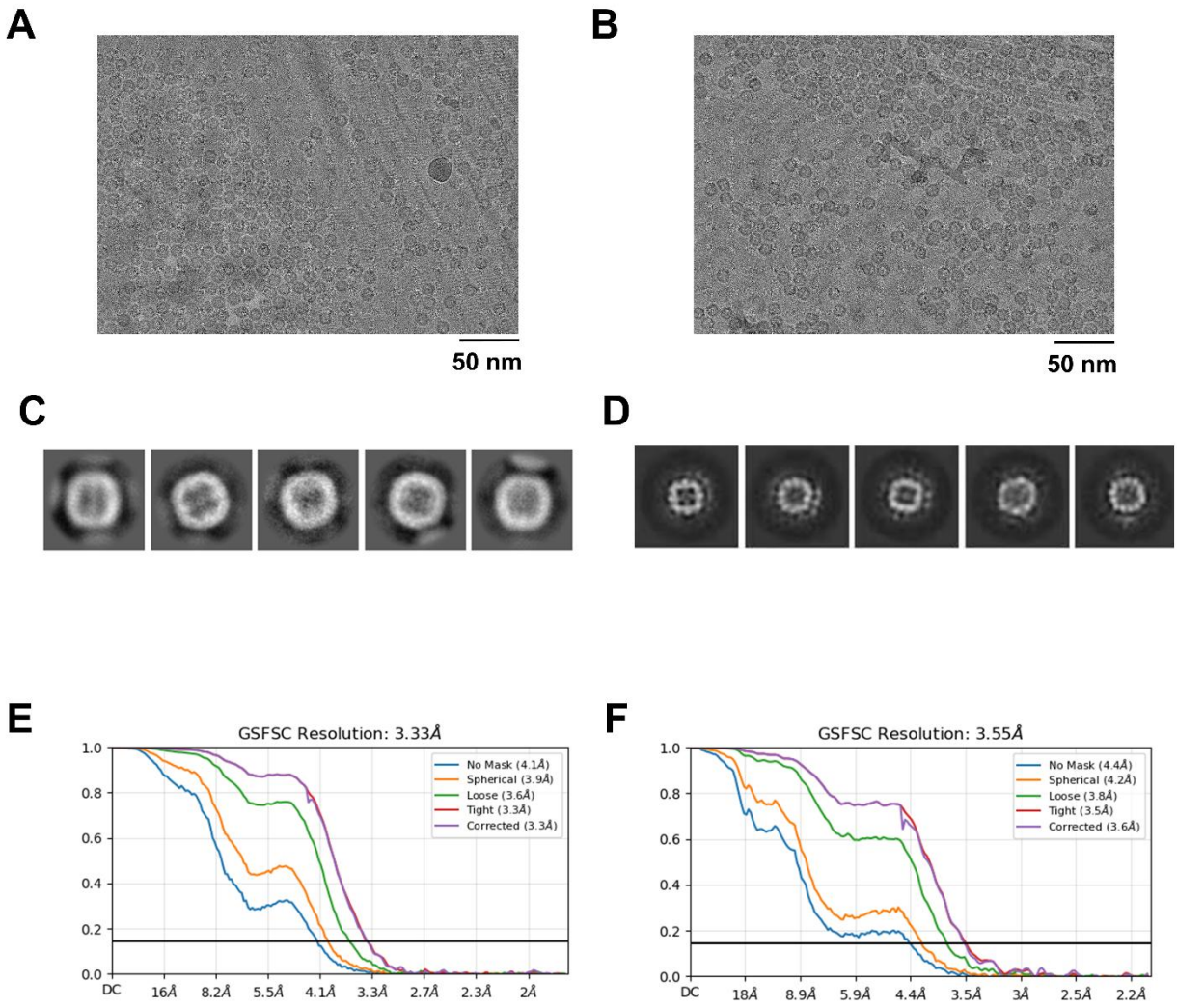


Figure 4. A) cryoEM images of apo Ferritin B) cryoEM images of Ferritin-adapter C) 2D averages of apo Ferritin D) 2D averages of Ferritin-adapter E,F) Fourier shell correlation (FSC) of the 3D reconstruction and FSC curves are plotted before and after masking. The black line represents the 0.143 FSC cutoff.

After 3D reconstruction, we interpreted the maps in ChimeraX using model-guided docking. The previously reported ferritin–NCOA4 complex structure (PDB: 8QU9) [17] was fitted into the cryo-EM maps, and a single FTH1 protomer was segmented for closer inspection. In the ferritin–fusion adapter map, density corresponding to the NCOA4 fragment was readily visible (shown in red). Outside this well-resolved region, only a small patch of additional density could be seen, likely corresponding to part of the GS linker; no interpretable high-resolution density attributable to the EGFR minibinder was observed. The most likely explanation is conformational heterogeneity: because the minibinder is

connected to NCOA4 through a flexible linker, it can sample multiple orientations relative to the ferritin surface, and that flexibility is averaged out during high-resolution reconstruction.

To examine the minibinder region more directly, we low-pass filtered both the apo ferritin and ferritin–fusion adapter maps to 10 Å. This suppresses high-resolution detail and makes low-resolution envelopes of flexible regions easier to interpret. Under these conditions, apo ferritin still showed no density outside the nanocage. By contrast, the ferritin–fusion adapter map displayed a clear additional density adjacent to the ferritin surface, and this feature could accommodate docking of the EGFR binder model. This supports assignment of the density to the minibinder module. Together, these cryo-EM observations provide structural evidence that the ferritin–fusion adapter complex assembles in vitro and suggest that linker rigidity will be an important variable in future optimization.

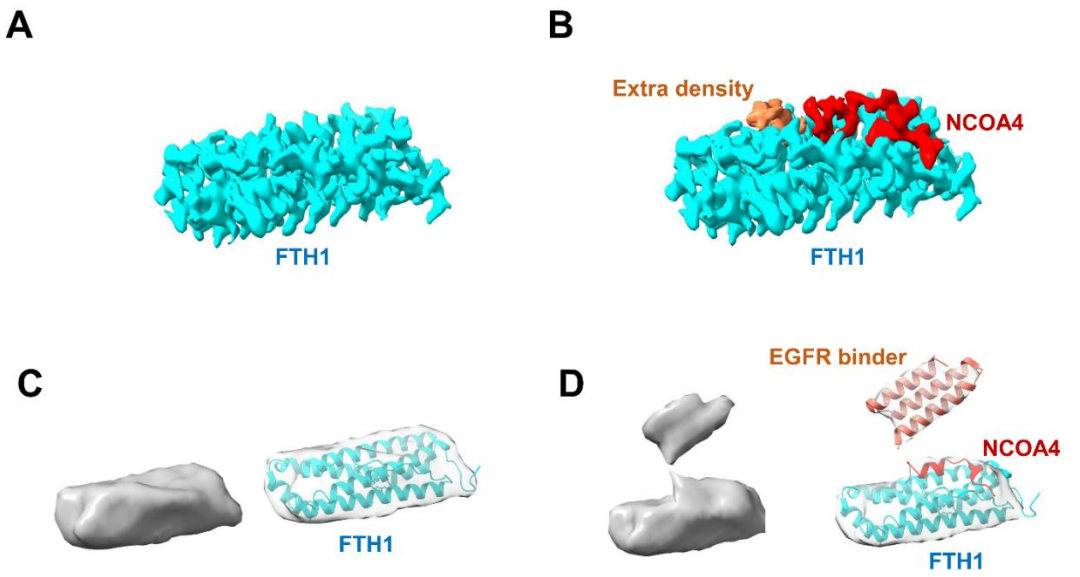


Figure 5. A) High resolution EM map of apo Ferritin. Ferritin is shown in cyan. B) High resolution EM map of Ferritin-adapter. Ferritin is shown in cyan, NCOA4 in red, and the extra density corresponding to the linker/binder region is shown in orange. C) Apo-ferritin EM map low-pass filtered to 10 Å resolution. The model of ferritin was docked into the density (right panel). The ferritin model is shown in cyan. D) Ferritin-adapter EM map low-pass filtered to 10 Å resolution. The models of ferritin, NCOA4, and the binder were docked into the density (right panel). The ferritin model is shown in cyan, the NCOA4 model in red, and the binder model in orange.

4. Conclusion

In summary, this study shows that ferritin nanoparticles can be functionalized through an exchangeable adapter while preserving native nanocage assembly. The main advance is the establishment of a modular design framework in which the targeting element can be modified without rebuilding the ferritin scaffold. Within the limits of the current data, we provide biochemical and structural support for this strategy in the context of EGFR-targeted applications relevant to GBM. These findings provide a useful basis for further development of ferritin-based targeting platforms.

5. Discussion

In this work, we established and experimentally validated an adapter-mediated strategy for assembling EGFR-targeted ferritin particles relevant to glioblastoma. The central point is not the discovery of a new biological interaction, but the demonstration that ferritin assembly and targeting-module design can be separated into two connected but independently tunable parts. Using FTH1 as the nanocage and an NCOA4–EGFR minibinder fusion as a bridge, we obtained biochemical and structural evidence that the assembled platform is stable in vitro. These data support adapter-mediated assembly as a practical framework for building ferritin-based targeting systems.

Ferritin has long been considered an attractive nanoscale carrier because of its defined architecture, stability, and biocompatibility. Most targeting strategies rely on direct surface modification, either through genetic fusion to ferritin subunits or chemical conjugation after assembly. Those routes can be effective, but they also tie ligand display closely to nanocage construction. Once the system has been built, further optimization often becomes cumbersome, especially when ligand size, spacing, or geometry needs to be adjusted. Chemical modification can also introduce variability in ligand number and orientation [18,19]. By contrast, the adapter-based strategy used here leaves the ferritin core unchanged and shifts most of the engineering burden to an exchangeable targeting module. This separation makes it easier to test alternative ligands without redesigning the nanocage itself.

Our data are consistent with earlier work showing that the C-terminal region of NCOA4 is sufficient for ferritin recognition [17]. In the context of the fusion construct, residues 475–511 still supported ferritin binding, even though the affinity was modestly weaker than that of the isolated NCOA4 fragment. This reduction likely reflects steric or conformational effects introduced by fusion to the EGFR minibinder, but the interaction remained in the same affinity range. At the same time, EGFR binding by the fusion adapter stayed close to reported values for the standalone minibinder, suggesting that the flexible GS linker largely preserved the function of both domains. Overall, the fusion design retained the expected behavior of each module while integrating them into a single assembly strategy.

Cryo-EM analysis provides a structural view of this assembly process. The NCOA4-derived region is well resolved and matches the previously described ferritin–NCOA4 interface, indicating that the engineered adapter preserves the native ferritin-binding mode. In contrast, the EGFR minibinder is not visible at high resolution, despite the biochemical evidence that it remains functional. The appearance of additional density only after low-pass filtering strongly suggests that the minibinder is present but conformationally mobile relative to the ferritin surface. This kind of behavior is common in cryo-EM studies of modular assemblies, where a flexible peripheral domain can be stably attached yet remain poorly resolved in the final reconstruction [20].

From an engineering standpoint, linker flexibility appears to be a key variable. A flexible linker is useful during initial construct design because it reduces steric interference and helps preserve the activity of each binding domain. At the same time, excessive flexibility can broaden the range of minibinder orientations, limit structural definition, and potentially affect how the ligand is displayed for multivalent receptor engagement. One obvious direction for future work is therefore to test partially rigid linkers or alternative adapter geometries that better control spatial presentation while maintaining binding.

This study also has several limitations. Most importantly, the work is confined to biochemical and structural validation; functional targeting, cellular uptake, and delivery performance were not examined here. In addition, linker flexibility prevented high-resolution visualization of the minibinder,

which limits detailed analysis of ligand orientation on the ferritin surface. Finally, although the measured affinities were favorable, further optimization of adapter stability and geometry will probably be needed before the platform can be evaluated under more complex biological conditions.

References

1. Wu W, Klockow JL, Zhang M, et al. Glioblastoma multiforme (GBM): An overview of current therapies and mechanisms of resistance. *Pharmacol Res.* 2021;171:105780.

2. Singh S, Dey D, Barik D, et al. Glioblastoma at the crossroads: current understanding and future therapeutic horizons. *Signal Transduct Target Ther.* 2025;10(1):213. Published 2025 Jul 9.

3. Rabah N, AitMohand FE, Kravchenko-Balasha N. Understanding Glioblastoma Signaling, Heterogeneity, Invasiveness, and Drug Delivery Barriers. Int J Mol Sci. 2023;24(18):14256.

4. Heimberger AB, Suki D, Yang D, Shi W, Aldape K. The natural history of EGFR and EGFRvIII in glioblastoma patients. *J Transl Med.* 2005;3:38.

5. Gan HK, Cvrljevic AN, Johns TG. The epidermal growth factor receptor variant III (EGFRvIII): where wild things are altered. FEBS J. 2013;280(21):5350-5370.

6. Li J, Liang R, Song C, Xiang Y, Liu Y. Prognostic significance of epidermal growth factor receptor expression in glioma patients. *Onco Targets Ther.* 2018;11:731-742.

7. Munro HN, Linder MC. Ferritin: structure, biosynthesis, and role in iron metabolism. *Physiol Rev.* 1978;58(2):317-396.

8. Sudarev VV, Dolotova SM, Bukhalovich SM, et al. Ferritin self-assembly, structure, function, and biotechnological applications. *Int J BiolMacromol.* 2023;224:319-343.

9. Mancias JD, Wang X, Gygi SP, Harper JW, Kimmelman AC. Quantitative proteomics identifies NCOA4 as the cargo receptor mediating ferritinophagy. *Nature.* 2014;509(7498):105-109.

10. Mancias JD, PontanoVaites L, Nissim S, et al. Ferritinophagy via NCOA4 is required for erythropoiesis and is regulated by iron dependent HERC2-mediated proteolysis. *Elife*. 2015;4:e10308.

11. Zhang B, Fan K. Design and application of ferritin-based nanomedicine for targeted cancer therapy. *Nanomedicine (Lond)*. 2025;20(5):481-500. doi:10.1080/17435889.2025.2459056

12. Zhen Z, Tang W, Chen H, et al. RGD-modified apoferritin nanoparticles for efficient drug delivery to tumors. *ACS Nano*. 2013;7(6):4830-4837. doi:10.1021/nn305791q

13. Wang, Y., Shi, L., Zou, C., Liu, Z., & Wang, J. (2025). Structural modification strategies for ferritin nanoparticles and their applications in biomedicine: a narrative review. *Nanoscale*, *17*(30), 17428–17442. https://doi.org/10.1039/d5nr01369k

14. Cao L, Coventry B, Goreshnik I, et al. Design of protein-binding proteins from the target structure alone. *Nature.* 2022;605(7910):551-560.

15. Watson JL, Juergens D, Bennett NR, et al. De novo design of protein structure and function with RFdiffusion. *Nature.* 2023;620(7976):1089-1100.

16. Xia Z, Jin Q, Long Z, et al. Targeting overexpressed antigens in glioblastoma via CAR T cells with computationally designed high-affinity protein binders. *Nat Biomed Eng.* 2024;8(12):1634-1650.

17. Hoelzgen F, Nguyen TTP, Klukin E, et al. Structural basis for the intracellular regulation of ferritin degradation. *Nat Commun*. 2024;15(1):3802. Published 2024 May 7. doi:10.1038/s41467-024-48151-1

18. Khoshnejad M, Parhiz H, Shuvaev VV, Dmochowski IJ, Muzykantov VR. Ferritin-based drug delivery systems: Hybrid nanocarriers for vascular immunotargeting. *J Control Release*. 2018;282:13-24. doi:10.1016/j.jconrel.2018.02.042

19. Lee NK, Cho S, Kim IS. Ferritin - a multifaceted protein scaffold for biotherapeutics. *Exp Mol Med*. 2022;54(10):1652-1657. doi:10.1038/s12276-022-00859-0

20. Bai XC, McMullan G, Scheres SH. How cryo-EM is revolutionizing structural biology. *Trends Biochem Sci*. 2015;40(1):49-57. doi:10.1016/j.tibs.2014.10.005

21. Zheng SQ, Palovcak E, Armache J-P, Verba KA, Cheng Y, Agard DA. MotionCor2: anisotropic correction of beam-induced motion for improved cryo-electron microscopy. Nat Methods. 2017;14(4):331-332. doi:10.1038/nmeth.4193

22. Punjani A, Rubinstein JL, Fleet DJ, Brubaker MA. cryoSPARC: algorithms for rapid unsupervised cryo-EM structure determination. *Nat Methods*. 2017;14(3):290-296. doi:10.1038/nmeth.4169

23. Abramson J, Adler J, Dunger J, et al. Accurate structure prediction of biomolecular interactions with AlphaFold 3. Nature. 2024;630(8016):493-500. doi:10.1038/s41586-024-07487-w